Hindawi
Journal of Nanomaterials
Volume 2018, Article ID 2789616, 14 pages
https://doi.org/10.1155/2018/2789616

Research Article

Anthocyanin-Sensitized TiO_2 Nanoparticles for Phenazopyridine Photodegradation under Solar Simulated Light

Ahed H. Zyoud,[1] **Fedaa Saleh**,[1] **Muath H. Helal**,[2] **Ramzi Shawahna**,[3] **and Hikmat S. Hilal**[1]

[1]*SSERL, Chemistry Department, An-Najah National University, Nablus, State of Palestine*
[2]*College of Pharmacy, An-Najah National University, Nablus, State of Palestine*
[3]*Department of Physiology, Pharmacology and Toxicology, Faculty of Medicine and Health Sciences, An-Najah National University, Nablus, State of Palestine*

Correspondence should be addressed to Ahed H. Zyoud; ahedzyoud@najah.edu

Received 25 September 2017; Revised 30 December 2017; Accepted 12 March 2018; Published 30 May 2018

Academic Editor: Mohamed Bououdina

Pharmaceutical wastes are emerging as water contaminants. Like other organic contaminants, it is necessary to find safe and economic methods to remove them from the water. In this work, anthocyanin was used as a natural dye sensitizer for the wide band gap nanosize rutile TiO_2. The TiO_2/*Anthocyanin* particles were supported on activated carbon particle surfaces. The resulting composite, which was prepared and characterized by different methods, was then used as a catalyst in the photodegradation of phenazopyridine (a model pharmaceutical contaminant) under a solar simulated light. Depending on experimental conditions, up to 90% of the contaminant was mineralized leaving no new organic products in the reaction mixture. The results show the feasibility of using the activated carbon-supported TiO_2/*Anthocyanin* photocatalyst for pharmaceutical contaminant removal in water. The natural dye anthocyanin readily sensitized the TiO_2 to visible light. The unsupported TiO_2, with its nanosize particles, was not easy to recover by simple separation methods, while the activated carbon-supported catalyst was easily isolated by decantation after reaction cessation. Moreover, the recovered AC/TiO_2 catalyst could also be regenerated by adding fresh anthocyanin sensitizer after recovery for further reuse. Keeping the contaminant molecules closer to the catalytic sites by adsorption, the support also enhanced the efficiency of photocatalyst.

1. Introduction

Natural waters are being contaminated with different organic compounds. Finding new ways to purify water is thus imperative. Different purification methods are used for this purpose, including physical, biological, and chemical processes [1–5]. Adsorption is another effective method commonly used in water purification [6, 7], but it has a shortcoming. The adsorbed contaminant molecules need further treatment or redesorption to recover the adsorbent material itself and to permanently remove the contaminant. Therefore, complete mineralization of the contaminant molecules should be targeted, and catalytic photodegradation needs to be considered for future water purification strategies. Advanced oxidation processes (AOPs) are emerging for water purification [8]. The AOP depends on the generation of highly reactive free radicals, such as the hydroxyl radical ($HO^{\bullet}$), which are effective in degrading organic contaminants [9]. The $HO^{\bullet}$ can be produced by different processes; one of which is photocatalysis with semiconductor and light. Palmisano and Sclafani defined photocatalytic degradation as *"A catalytic process during which one or more reaction steps occur by means of electron-hole pairs generated on the surface of semiconducting materials when illuminated by a light of suitable energy"* [10].

TiO_2 is the most commonly used semiconductor in water purification due to its high stability, nontoxic nature, high oxidizing potential, insolubility in water under different conditions, and low cost. Rutile is the most stable form of TiO_2, whereas anatase is the most catalytically active system [11, 12] due to its more negative flat band potential than rutile.

This makes the anatase more competitive than rutile for the reduction reaction. Rutile is thus intentionally chosen here for reasons discussed below.

TiO_2 is activated by UV light at wavelengths shorter than 387 nm. When TiO_2 particle absorbs a photon having energy greater than the band gap (E_{bg}), the electron in the valence band (VB) will be excited to the conduction band (CB). The result of such excitation will be electron-hole pair formation [11, 13].

The hole, formed as a result of electron excitation, has a potential to oxidize water by forming a hydroxyl radical ($OH^{\bullet}$). The electrons in CB readily reduce oxygen to form the superoxide anion. This can, in turn, react with water to form hydroxyl radical again. Hydroxyl radicals are very powerful oxidizers and can easily oxidize an organic species ultimately to carbon dioxide, water, and other less hazardous minerals.

The oxidation of organic compounds may occur as described in the following equation [14]:

$$OH^{\bullet} + O_2 + C_nO_mH_{(2n-2m+2)} \longrightarrow nCO_2 + (n - m + 1)\,H_2O \quad (1)$$

For efficient photocatalysis to occur in a given catalytic mixture, the pollutant should be adsorbed or should be very close to the catalyst surface. When the surface area increases the number of adsorbed molecules should also increase. Nanoparticles have relatively high relative surface areas, compared to macrosystems. Therefore nanoparticles are very efficient photocatalysts. In this work, smaller nanosize rutile TiO_2 particles (the most stable TiO_2 type) will be prepared and examined. With a wide band gap (3.2 eV) TiO_2 may not be effective in degradation of organic compounds, due to low abundance of UV in the oncoming solar light [15, 16], as only ~4-5% of the incoming solar light belong to the UV region [17, 18]. To efficiently utilize solar energy, the catalyst must be modified to absorb in the visible region. Different methods were followed to achieve this. Doping TiO_2 with another element, such as nitrogen, to reduce the band gap energy is one method [19, 20].

Another way is to sensitize the wide gap semiconductors to visible light. Narrow band gap semiconductors like CdS have been described as sensitizers and as photocatalysts in water purification [21–23]. CdS dye absorbs in the visible region and enhances TiO_2 photocatalyst efficiency, but unfortunately yields the hazardous Cd^{2+} ions in solution upon dissolution [21].

Most of the advanced oxidation processes need UV light, and some processes need to use metal like Fenton reaction that has bad effects on the human body in addition to its cost [14].

Dye molecules, such as transition heavy metal compounds, are also used to sensitize TiO_2. Light absorption occurs by the dye molecule that is attached to the TiO_2 nanoparticle, in the visible region. When the dye molecule absorbs a photon, its electron will be excited from HOMO (Highest Occupied Molecular Orbital) level to LUMO (Lowest Unoccupied Molecular Orbital) level. This is followed by relaxation through electron loss to the TiO_2 conduction band [24]. Despite their advantages, synthetic metal based dyes may readily decompose in the solution under the working conditions. Sensitization by natural dyes is thus the alternative sensitizer in photodegradation of aqueous organic contaminants [25, 26].

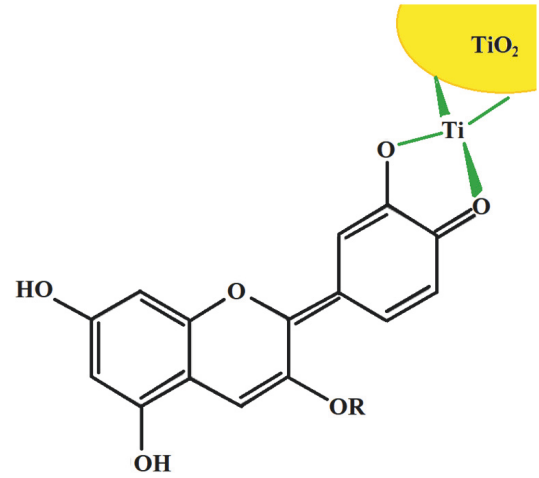

Scheme 1: Structural formula of anthocyanin molecule attached to TiO_2.

The main purpose of this work is to prepare a stable, active, easy to use photocatalyst that can be excited with visible light. Due to its stability [27], rutile was intentionally chosen here as the catalyst. As a challenge, its low efficiency will be enhanced by sensitization as described here. Anthocyanin will be used as a natural dye sensitizer. Such a dye is safe, abundant, cheap, and contains α-hydroxyl carbonyl group to attach to the TiO_2 surface, as shown in Scheme 1. Natural dye sensitizers have been commonly reported in solar cell applications, but to a much lesser extent for water purification [28, 29]. Very few reports in using natural dye sensitized catalysts are known [25, 26, 30]. Anthocyanins are stable water-soluble pigments that widely occur in nature. The pigment can be extracted from flowers of a plant called Karkade (Hibiscus). Karkade is commonly abundant at market-places and is used as a safe low cost beverage in different Middle East regions. Anthocyanin contains hydroxyl groups (OH). It may then keep the catalyst surface hydrophilic, which would keep the water contaminants closer to the catalyst surface and lower the tension between the catalyst surface and the aqueous solution [31–34]. The dyes are responsible for the red, blue, and purple colors of many plants [35]. Due to its OH groups, the dye may chemisorb with TiO_2 surface [36–38].

Phenazopyridine, 2,6-diamino-3-(phenylazo) pyridine, is a widely used drug. Its structure is shown in Scheme 2. Its removal from water will be examined here by photodegradation. This strategy is important for further practices aiming at purifying water from pharmaceutical wastes that are commonly found in the environment [39–42].

As the TiO_2 used here is in the nanoscale, it is difficult to recover from the reaction medium by simple separation methods. Therefore, it is necessary to facilitate the catalyst recovery and to increase the effective catalyst surface area

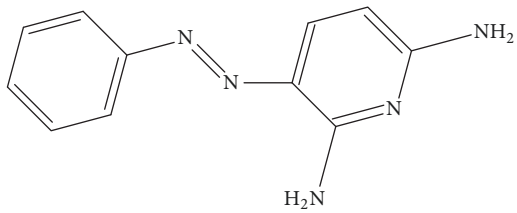

Scheme 2: Structural formula for phenazopyridine.

as well. For these purposes, activated carbon (AC) particles, which are hydrophilic in nature, are used here as support (not dopant) for the TiO_2 nanoparticles. In addition to that, AC has high adsorption capacity which keeps the contaminant molecules closer to the catalyst surface and consequently increases the photodegradation rate. These findings, parts of which are based on Saleh thesis [43], are described below.

2. Experimental

2.1. Chemicals and Equipment. All starting chemicals, acids, bases, and organic solvents were purchased in pure form from Sigma-Aldrich, Merck. Commercial TiO_2 was purchased from Aldrich (99.5% pure, Model number *637262*, with particle size ~100 nm). The commercial TiO_2 was used only for comparison purposes in characterization study as described below.

A Shimadzu UV-1601 spectrophotometer was used for electronic absorption spectra measurements. A Perkin Elmer LS 55 Luminescence Spectrometer was used for photoluminescence measurements. A Philips XRD X'PERT PRO diffractometer with Cu Ka (λ = 1.5418 Å) was used for XRD measurements. A Jeol-EO Scanning Electron Microscope was used for SEM imaging. AThermo Scientific™ Nicolet™ iS™5 FT-IR Spectrometer was used for FT-IR measurements. A Hitachi Model S-4300 Field Emission Scanning Electron Microscope was used for electron dispersion X-ray (EDX) spectra measurement at Korea. A TA 2950HR V5-3 TGA apparatus was used for thermogravimetric analysis at ICMCB, University of Bordeaux, France.

2.2. Catalyst Preparation

2.2.1. Extraction of Anthocyanin Dye. A 30 g commercial *roselle (Hibiscus sabdariffa)* dried flowers were crushed and soaked in a 500 ml Erlenmeyer flask with 300 ml of methanol. The mixture was acidified with few drops of HCl and magnetically stirred at room temperature for 1 hr. The concentration was measured spectrophotometrically using the molar absorptivity, $\varepsilon = 37200\ \text{L mol}^{-1}\ \text{cm}^{-1}$, and found to be 5×10^{-4} M. The solution was then filtered and transferred into a dark color glass bottle for further use [45, 46].

2.2.2. Preparation of AC/TiO_2/Anthocyanin. A $TiCl_3$ (50 mL, ~10%) solution was placed in a 250 mL conical flask. NaOH (100 ml, 2.5 M) was then added dropwise with continuous stirring until a white suspension powder appeared. The resulting TiO_2 powder was then decanted and washed with water 2 times [47]. A small portion of the suspension was centrifuged (5000 rpm), and the isolated powder was left to dry at room temperature and kept for further characterization.

The TiO_2 particle suspension (150 mL) was mixed with activated carbon (2.0 g) and stirred for an hour, and the mixture was then filtered and dried in an oven at 130°C. Alcoholic extract of anthocyanin (100 mL, 5×10^{-4} M) was added to the resulting dried *AC/TiO_2* powder (10 g) and stirred for an hour. The mixture was then filtered, and the solid was left to dry at room temperature. The resulting *AC/TiO_2/Anthocyanin* system was stored in the dark for further use.

2.3. Photocatalytic Experiments. Catalytic experiments were conducted in a thermostated magnetically stirred 100 mL beaker. The walls of the beaker were covered with aluminum foil to reflect back any stray radiation. An aqueous solution (50 mL) of known phenazopyridine concentration and a specific amount of catalyst were placed in the beaker. The required pH value was controlled by adding drops of NaOH or HCl dilute solutions. Direct visible irradiation of solar simulator halogen spot lamp ($1.9 \times 10^{-4}\ \text{W/cm}^2$) was placed vertically above the photocatalytic reaction mixture. Small aliquots of solution were syringed out from reaction vessel at different reaction periods, centrifuged (5000 rpm) for 5 minutes. The supernatant (0.100 mL) was added to 5 mL Britton-Robinson buffer solution (pH 8) and then analyzed for remaining contaminant by differential anodic stripping voltammetry technique using POL 150 Polarograph with a hanging drop mercury electrode (MDE 150) [48].

2.4. Control Experiments. Several control experiments were conducted. Firstly, a mixture of phenazopyridine solution (50 mL) and *AC/TiO_2/Anthocyanin* (0.1 g) was stirred in dark, to check the amount of contaminant adsorbed on catalyst system surfaces. The mixture reached adsorption equilibrium after 120 min. To account for the adsorbed contaminant in later photocatalytic reaction experiments, the mixture of the contaminant with catalyst was stirred in the dark for at least 120 min, before exposure to light.

Secondly, in the absence of any catalyst, a stirred contaminant solution (50 ml) was exposed to solar simulated light for 100 min. The phenazopyridine concentration was measured before and after exposure to light, to check for any phenazopyridine loss by light (photolysis) with no catalyst. Thirdly, a control experiment with a cut-off filter (blocking 400 nm and shorter wavelengths) placed between the reaction surface and the light source confirmed the ability of anthocyanin to sensitize TiO_2 in visible light with waves longer than 400 nm. Control experiments using the cut-off filter were performed for *naked TiO_2*, *AC/TiO_2/Anthocyanin*, and *AC/TiO_2*, as discussed below.

Effects of containment concentration, catalyst type and amount, and pH on the photodegradation process were all studied. For efficiency comparison, values of reacted contaminant molecules per incident photon (quantum yield, QY) and values of reacted contaminant moles per nominal TiO_2 mole (turnover number, TN) were calculated after 60 min in each experiment.

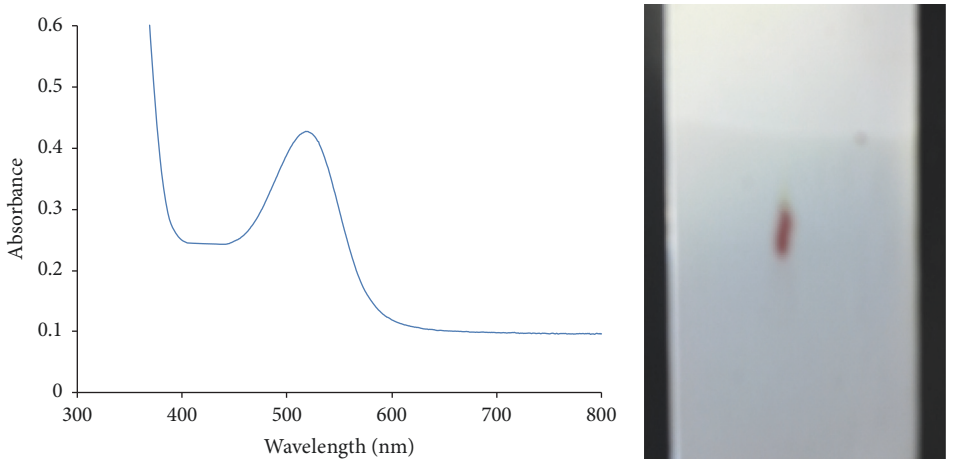

Figure 1: Electronic absorption spectra (a) and TLC (b) for the extracted anthocyanin dye.

2.5. Catalyst Stability Experiments. Solutions (50 mL, 2×10^{-5} M) of anthocyanin were adjusted to pH ranging 3 or 9. To each solution was added 0.1 g *AC/TiO$_2$/Anthocyanin*, and the suspension was stirred for 120 min. The reaction mixture was then exposed to the light source with stirring for 100 min with and without a cut-off filter. For control purposes, the anthocyanin UV-visible absorption spectrum was measured before and after exposure to light. This was to examine the stability of anthocyanin itself under photodegradation conditions.

The FT-IR spectra were measured for *Anthocyanin* solution, *AC/TiO$_2$*, and *AC/TiO$_2$/Anthocyanin* before and after photocatalytic experiments. This was to test the presence of adsorbed anthocyanin remaining on the catalyst surface after photodegradation reaction cessation.

2.6. Catalyst Recycling and Regeneration. To examine the efficiency of the catalyst after recovery, a solution (50 mL, 40 ppm) of phenazopyridine was stirred 120 min in dark with 0.2 g *AC/TiO$_2$/Anthocyanin* at pH = 9. The solution was then exposed to light for 100 min. The phenazopyridine concentration was measured before and after light exposure. The solution was then decanted leaving the catalyst in the container, and another fresh contaminant solution (50 mL, 40 ppm) of phenazopyridine was added to the container, with pH = 9. The fresh solution was stirred in dark for 120 min and then exposed to light for 100 min. The phenazopyridine concentration was measured before and after light exposure. The recycling experiments were also performed after regenerating the catalyst with fresh anthocyanin dye. Catalyst regeneration was also examined after decantation by adding a 2 mL of anthocyanin solution to the stirred catalyst suspension for 30 min. The catalyst was then decanted and washed with fresh water.

3. Results and Discussion

3.1. Catalyst Characterization. Different techniques were used to characterize the prepared sensitized catalyst. The electronic absorption spectrum and thin layer chromatography (TLC) for extracted anthocyanin solution are shown in Figure 1. The spectrum shows a typical absorption band at $\lambda_{max} \sim 540$ nm, and the TLC shows that the extracted solution involves one component. Based on the reported absorptivity in 1% HCl/ethanol ($\varepsilon = 37200$ L mol^{-1} cm^{-1}) the anthocyanin calculated concentration in the solution was 5×10^{-4} M, as shown above.

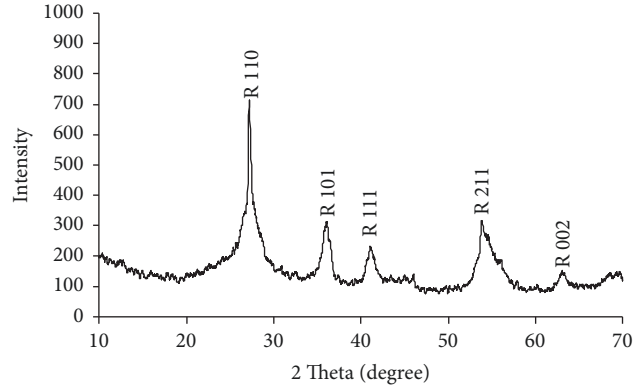

Figure 2: XRD pettern of TiO$_2$ nanopowder.

The XRD patterns were measured for the prepared TiO$_2$ nanoparticles, Figure 2. By comparison with rutile TiO$_2$ standard card (00-001-1292), the XRD pattern showed that the prepared TiO$_2$ powder was rutile form. The particle size of the prepared TiO$_2$ powder was calculated by Scherrer equation based on XRD pattern and was found to be ~37 nm.

Scanning electron micrography (SEM) was used to study the surface morphology of the prepared sample. SEM image, Figure 3, shows that the TiO$_2$ involved large agglomerates (>500 nm) of TiO$_2$ with smaller nanosize particles of less than 50 nm size, while the AC/TiO$_2$ involved smaller aglomerates (~300 nm) of TiO$_2$ with smale nanoparticle size (~20 nm). Based on XRD and SEM results, the TiO$_2$ involves nanosize

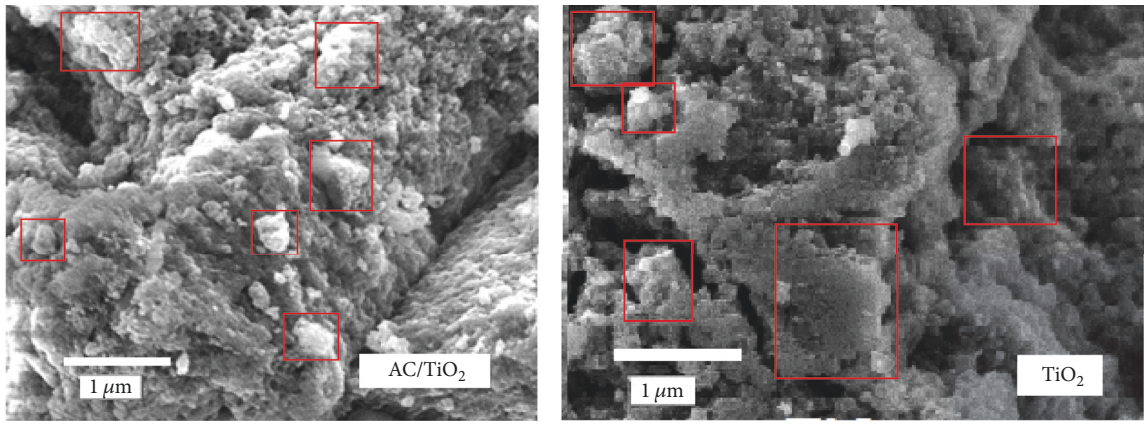

Figure 3: SEM image of TiO_2 nanopowder supported on AC and TiO_2 nanopowder alone.

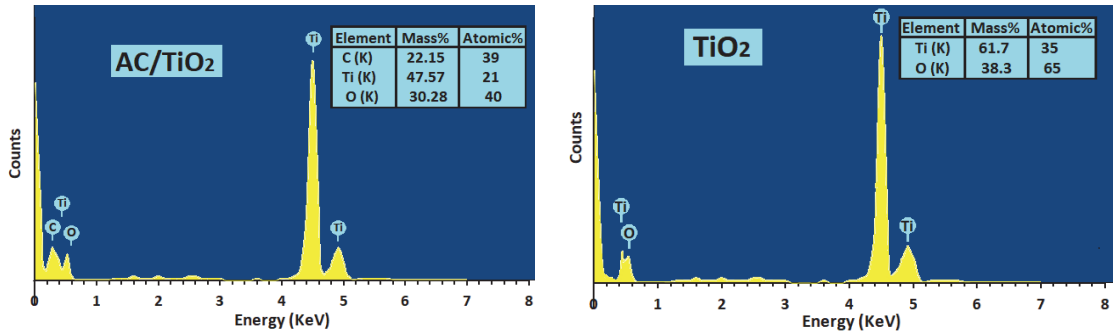

(a) (b)

Figure 4: EDX spectra measured for (a) AC/TiO_2, and (b) TiO_2.

particles that live inside larger agglomerates. The SEM results are consistent with the XRD results with respect to the nanosize nature of the TiO_2 particles living inside agglomerates.

Energy Dispersive X-Ray (EDX) analysis for AC/TiO_2 and TiO_2 was measured. The results are shown in Figure 4. The EDX results show that the atomic ratio for the prepared TiO_2 is approximately (Ti : O) 1 : 2, and the mass ratio between AC and TiO_2 is approximately 22 : 78.

Figure 5 shows the thermogravimetric analysis (TGA) plot for the composite AC/TiO_2. The TGA results confirm that the TiO_2 mass is ~78% in the composite catalyst, and the AC is ~22%. The TAG analysis ratio between AC and TiO_2 is consistent with EDX analysis result.

Photoluminescence (PL) spectra were measured for the prepared TiO_2 nanopowder, as shown in Figure 6. The prepared powder shows similar PL spectrum with the rutile type [49, 50]. Commercial TiO_2 was used here as a benchmark only. The observed slight blue shift in the prepared particles, compared to the commercial ones, is attributed to the smaller size of the former nanosize particles. The photoluminescence spectrum for the TiO_2 in the AC/TiO_2 is similar to that of naked TiO_2.

The solid electronic absorption spectrum for *TiO_2/Anthocyanin* was measured using a suspension of a specific amount of the catalyst in toluene. The absorption spectrum is shown

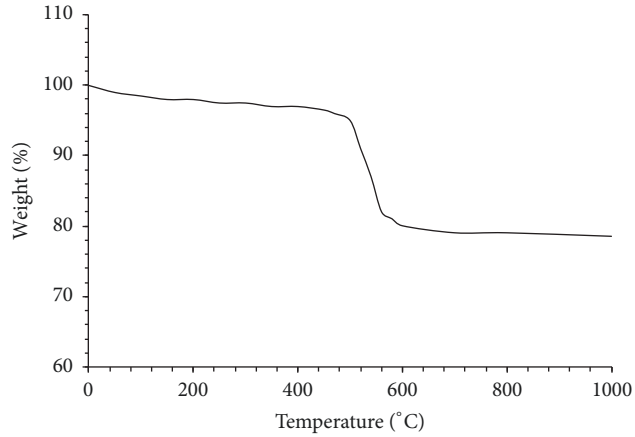

Figure 5: The TGA profile of AC/TiO_2 composite. Loss of activated carbon occurs in the temperature range 500–600°C.

in Figure 7. The figure shows two absorption peaks, the first at ~400 nm is attributed to TiO_2, and the second at ~600 nm is attributed to anthocyanin attached molecules.

The detailed characterization discussions shown above thus confirm the rutile nature of TiO_2 in different catalytic

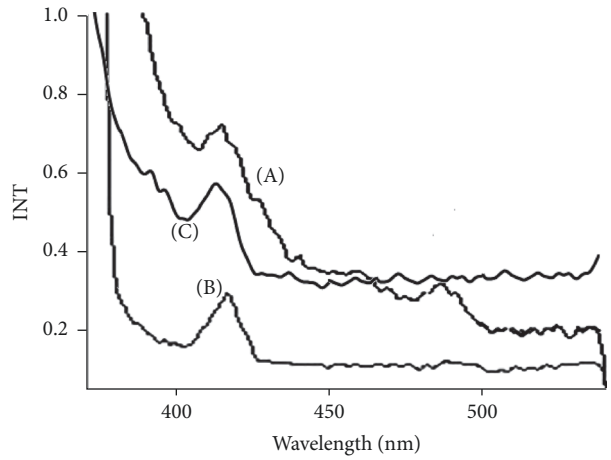

Figure 6: Photoluminescence spectra measured for rutile TiO_2: (A) prepared, (B) commercial TiO_2 samples, and (C) AC/TiO_2. All spectra were measured as suspensions using excitation wavelength λ_{ex} = 360 nm.

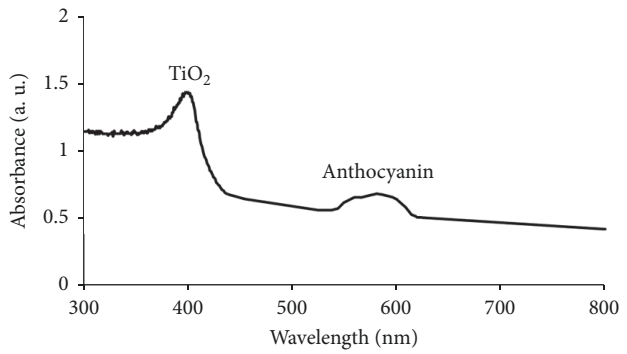

Figure 7: Solid state electronic absorption spectra measured for *TiO_2/Anthocyanin*.

systems examined here. A general description for each solid is shown again for quick comparison in Table 1. Details of efficiency for each solid are described in Section 3.

3.2. Control Experiment Results. As stated above, control experiments were conducted to confirm the role of *AC/TiO_2/Anthocyanin* system as a catalyst in photodegradation of phenazopyridine. When the phenazopyridine solution was irradiated in the absence of any catalyst, no decrease in contaminant concentration was observed for more than 120 min. This means that the contaminant did not degrade in the absence of catalysts (no photolysis). When anthocyanin was added alone to the phenazopyridine, no significant loss in phenazopyridine concentration was observed after irradiation with visible or solar simulated light for 120 min. Using *naked TiO_2* with cut-off filter shows no significant loss in phenazopyridine, which means that the naked TiO_2 does not function in the visible light.

When *AC/TiO_2/Anthocyanin* system was added to the phenazopyridine solutions (40 ppm) in the absence of light, contaminant concentration continued to decrease until it reached a constant equilibrium value (~15 ppm) after 120 min. The contaminant concentration reduce is due to adsorption onto the *AC/TiO_2/Anthocyanin*. These observations were taken into consideration when using the *AC/TiO_2/Anthocyanin* system in photodegradation experiments of phenazopyridine, taking into the account the adsorbed ~25 ppm loss by adsorption on the catalyst surface.

When a cut-off filter was used, in the presence of *AC/TiO_2/Anthocyanin,* a significant loss in the phenazopyridine concentration occurred due to photocatalysis. No observable loss in phenazopyridine occurred when using a cu-off filter in case of *AC/TiO_2* system (nonsensitized). These results confirm the ability of anthocyanin to sensitize TiO_2 in photodegradation of phenazopyridine under visible light. In this technique, light absorption occurs by the dye molecule that is attached to the TiO_2 nanoparticle, in the visible region, as summarized in Scheme 3.

When the dye molecule absorbs a photon, one electron will be excited from its HOMO to LUMO. This is followed by relaxation through electron loss to the TiO_2 CB [24]. Hole in the HOMO of dye will produce the active species ($^{\bullet}OH$) which leads to oxidation of the organic species; spontaneously the electrons in the conduction band of the TiO_2 will reduce other species (like O_2) or other contaminant cations. Literature confirmed the formation of the $^{\bullet}OH$ active species during the photodegradation processes, and their roles in oxidizing contaminant molecules to CO_2, H_2O, and other mineral species like SO_3^{-2}, SO_4^{-2}, NH_4^{+}, and NO_3^{-} [9, 51–53]. For electron relaxation to occur, the energy level of the LUMO must be higher than the conduction band edge of TiO_2, so that an electron can be injected during the relaxation process. The dye HOMO must also be lower (more positive) than the reduction potential of the organic contaminant.

3.3. Photocatalytic Experiment Results. Contaminant adsorption onto solid catalysts was confirmed by mixing the contaminant solution with catalyst in the dark for 120 min. After that, the reaction mixture was exposed to light, and the photocatalytic reaction profiles were then monitored from that moment. The phenazopyridine photodegradation reaction was studied using *AC/TiO_2/Anthocyanin* system in water.

In photocatalytic experiments, the loss of phenazopyridine is due to photodegradation. This was confirmed by additional control experiments. In case of dark adsorption study, the adsorbed phenazopyridine molecules desorbed by treating the saturated solid system with an organic solvent like DMSO. After photocatalytic experiment completions, treating the remaining solid material did not show significant contaminant molecule desorption when treated with dimethyl sulfoxide (DMSO). These results confirm the mineralization of the contaminant molecules adsorbed onto the solid material during photocatalysis experiments.

Effects of different reaction parameters, such as pH, temperature, catalyst concentration, and contaminant concentration, on the rate of photodegradation reaction, were all studied as shown in Figures 8–11. Values of degradation percentage, turnover number (TN, reacted phenazopyridine molecules/TiO_2 molecules), turnover frequency (TF, reacted phenazopyridine molecules/TiO_2 molecules per unit time),

Table 1: General description for different TiO_2 solid systems examined as photodegradation catalyst.

	Commercial TiO_2	Lab prepared TiO_2	AC/TiO_2	AC/TiO_2/Anthocyanin
Preparation method	Hard-templating technique	Sol-gel	Sol-gel precipitation onto AC	Chemisorption of dye onto AC/TiO_2 solid
TiO_2 Particle size	~100 nm	~37 nm Inside larger agglomerates	~37 nm Inside larger agglomerates	~20 nm Inside larger agglomerates
Band gap value (based on PL and absorption spectra)	3.0 eV	~3.05 eV	~3.05 EV	~3.05 eV for TiO_2 (2.13 eV for anthocyanin)
Photo-catalytic efficiency under UV	-	Effective	Effective	Effective
Photo-catalytic efficiency under visible	-	Non-effective	Non-effective	Effective
TiO_2 stability under reaction	-	Stable	Stable	Stable (Dye degrades; can be regenerated)

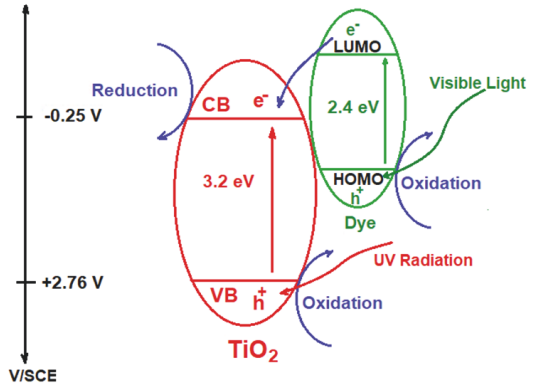

Scheme 3: A schematic showing sensitization of TiO_2 in photodegradation.

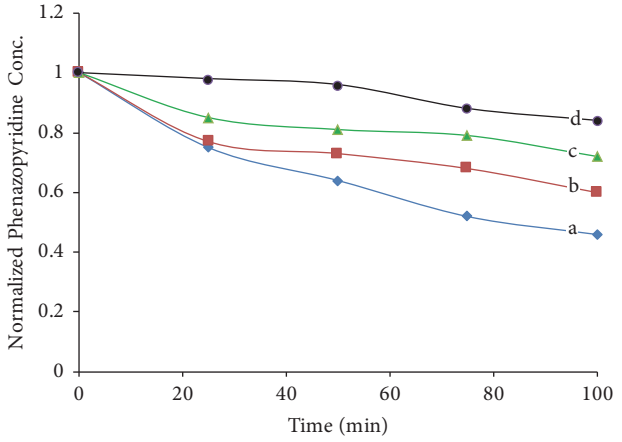

Figure 8: Effect of pH on phenazopyridine photodegradation progress: (a) pH = 9, (b) pH = 7, (c) pH = 5, and (d) pH = 3.

and quantum yield (QY, reacted phenazopyridine molecules/incident photon) are summarized in Table 2.

3.3.1. Effect of pH. The pH value is an important variable in photodegradation reactions. That is because it influences the surface electric charges of TiO_2 catalyst [54]. The point of zero charge of TiO_2 (pH_{pzc}) is close to pH 6.8. At values higher than pH_{pzc}, the surface of TiO_2 becomes negatively charged as ($TiOH + OH \rightleftharpoons H_2O + TiO^-$). When the pH value is lower than pH_{pzc} the surface of TiO_2 becomes positively charged as follows ($TiOH + H^+ \rightleftharpoons Ti - OH_2^+$), [55]. Anthocyanin is more stable in acidic media. The dynamic equilibria for anthocyanin at different pH values are shown in Scheme 4.

In acidic media (pH ~ 0.5) the red flavylium cation is the major equilibrium species. When pH is higher the color intensity decreases and the concentration of flavylium cation is lowered as shown in Scheme 4. When anthocyanin chelates to TiO_2 its stability increases even at higher pH [44]. The effect of pH on the photodegradation of phenazopyridine was examined on four solutions of phenazopyridine (40 ppm each). The solutions were adjusted to different pH values (3, 5, 7, 9), under stirring with 0.1 g catalyst for 120 min in dark before exposure to the light source. The photodegradation profiles of phenazopyridine at different pH values are shown in Figure 8.

Table 2: Phenazopyridine photodegradation results represented in % degradation, turnover number (TN, molecules/ZnO unit), turnover frequency (TF, min^{-1}), and quantum yield (QY, molecules/photon).

Effect of pH on phenazopyridine photo-degradation progress				
pH	3	5	7	9
% degradation	15%	26%	40%	54%
TN	4.8×10^{-4}	7.9×10^{-4}	10.0×10^{-4}	16.0×10^{-4}
TF	4.8×10^{-6}	7.9×10^{-6}	10.0×10^{-6}	16.0×10^{-6}
QY	4.4×10^{-3}	7.1×10^{-3}	7.3×10^{-3}	14.5×10^{-3}
Effect of contaminant concentration on the photo-degradation progress				
Contaminant ppm	30	35		40
Init. Conc., ppm	9.7	12.5		15.5
Final conc., ppm	6.5	9		12
% degradation	33%	28%		23%
TN	8.0×10^{-4}	8.9×10^{-4}		9.0×10^{-4}
TF	8.0×10^{-6}	8.9×10^{-6}		9.0×10^{-6}
QY	5.8×10^{-3}	7.8×10^{-3}		8.1×10^{-3}
Effect of temperature on the photo-degradation progress				
Temperature. ˚C	15	25	35	45
% degradation	8.5%	14%	20%	33%
TN	2.98×10^{-4}	4.93×10^{-4}	7.46×10^{-4}	11.2×10^{-4}
TF	2.98×10^{-6}	4.93×10^{-6}	7.46×10^{-6}	11.2×10^{-6}
QY	2.7×10^{-3}	4.5×10^{-3}	6.8×10^{-3}	10.2×10^{-3}
Effect of catalyst amount on the photo-degradation progress				
Catalyst, g	0.050	0.075		0.150
% degradation	29%	50%		88%
TN	4.93×10^{-4}	5.44×10^{-4}		8.86×10^{-4}
TF	4.93×10^{-6}	5.44×10^{-6}		8.86×10^{-6}
QY	4.5×10^{-3}	4.9×10^{-3}		7.9×10^{-3}

All values of degradation percentage, turnover number (TN), turnover frequency (TF), and quantum yield (QY) increased with higher pH value, Table 2. The catalyst efficiency is thus higher at higher pH values. Literature shows that in some cases photodegradation reactions become faster at higher pH [56] while in other cases the reactions (of other compounds) became slower [57, 58].

Based on the point of zero charges of TiO_2 (pH_{pzc}), the TiO_2 surface is positively charged, whereas at higher pH the surface is negatively charged. On the other hand, at lower pH values, the contaminant phenazopyridine gains positive charges [44, 55, 56]. As a base, phenazopyridine retains its neutral charge at higher pH. This explains the effect of pH on phenazopyridine degradation here. At lower pH values, both TiO_2 and phenazopyridine are positively charged, which lowers adsorption of the latter onto the former. At higher pH, TiO_2 surface carries a negative charge, which attracts the partial positive charge present onto H-atoms of the amine group of neutral phenazopyridine. These discussions are explained in Scheme 5. As adsorption increases, with higher pH, the photocatalytic efficiency is expected to increase. Moreover, anthocyanin shows higher stability in alkaline media pH (8-9) than under nearly neutral conditions [59, 60] which retains the sensitizer activity at higher pH.

3.3.2. Effect of Contaminant Concentration. Effect of contaminant concentration on phenazopyridine photodegradation progress was studied. Different contaminant nominal concentrations (30, 35, and 40 ppm) were used. As stated above, when the catalytic reaction mixture was left in the dark for 120 min, contaminant adsorption occurred. After equilibrium was reached, the initial remaining contaminant concentrations, before photodegradation started, were measured to be 10, 13, and 16 ppm. Figure 9 shows reaction profiles for normalized remaining contaminant concentrations with time. The photodegradation percentage is higher for lower nominal contaminant concentrations.

Table 2 shows that phenazopyridine photodegradation percentage decreased as contaminant initial concentration was increased. This should not be considered as an indication of catalyst efficiency lowering. Values of quantum yield increased with increasing contaminant concentration. Moreover, the values of catalyst TN and TF also increased with higher contaminant concentration. Collectively, the

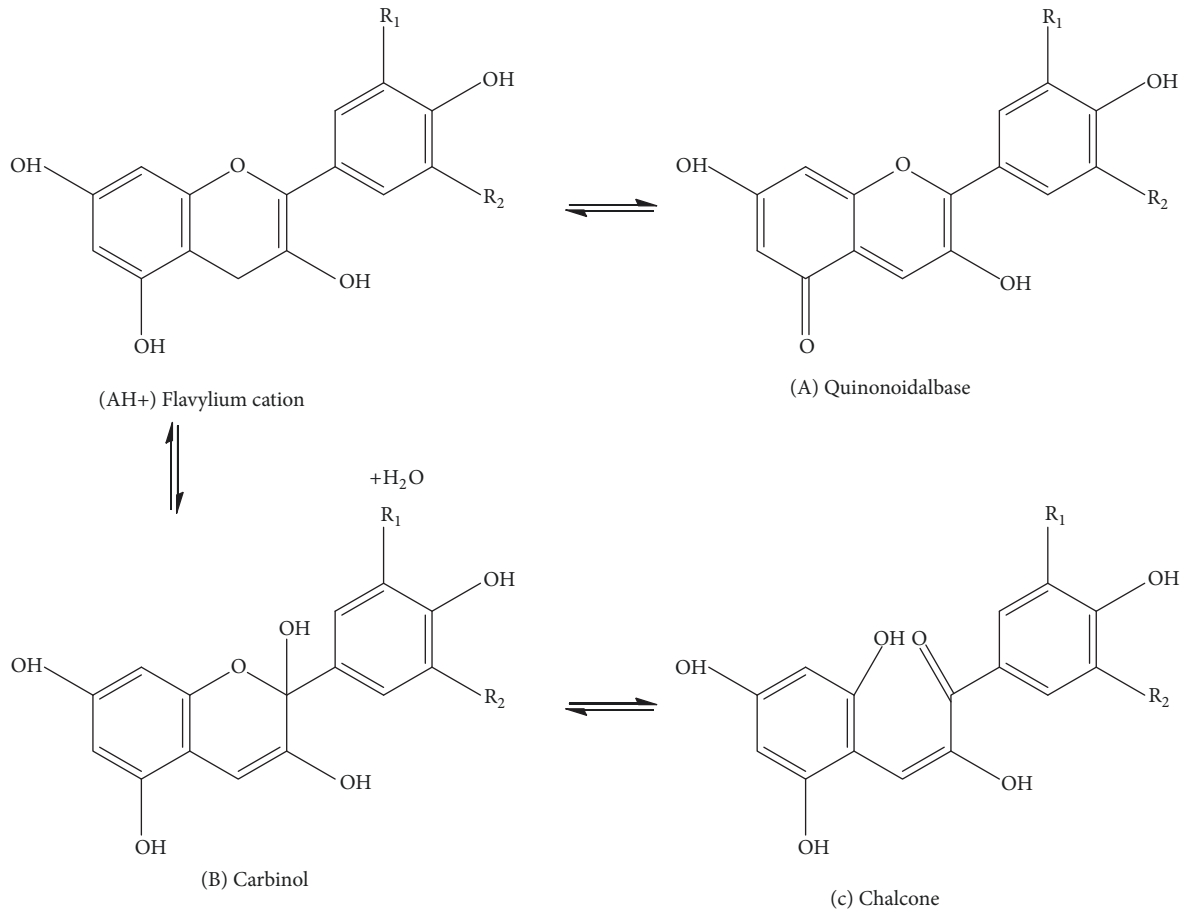

Scheme 4: Different forms for anthocyanin at different pH ranges [44].

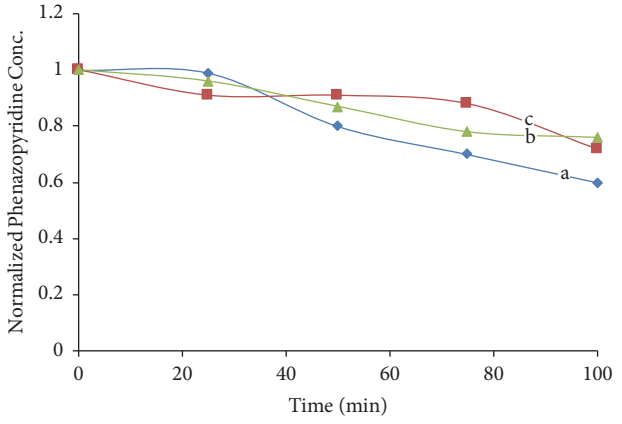

Figure 9: Effect of contaminant concentration on photodegradation reaction progress. All reactions were conducted at room temperature using contaminant concentration: (a) 30 ppm, (b) 35 ppm, and (c) 40 ppm.

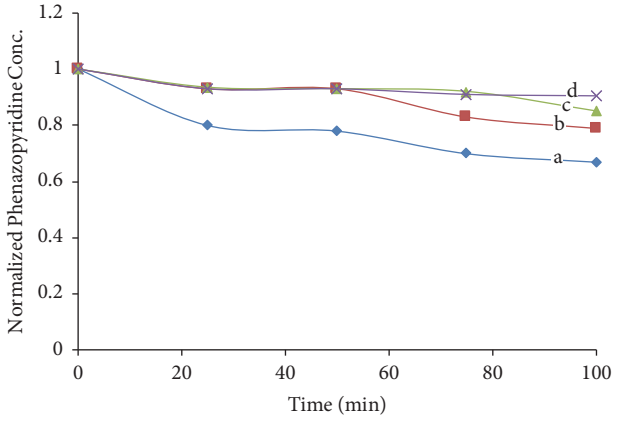

Figure 10: Effect of temperature on phenazopyridine photodegradation reaction: (a) 45°C, (b) 35°C, (c) 25°C, and (d) 15°C.

results indicate that the catalyst efficiency is higher with higher initial contaminant concentration. These results are consistent with earlier studies using ZnO catalyst [54, 61].

3.3.3. The Effect of Temperature. Effect of temperature on phenazopyridine photodegradation progress was studied here. Different temperatures (15, 25, 35, and 45°C) were used for photodegradation of 50 mL phenazopyridine solution (40 ppm) mixed with 0.1 g catalyst. Figure 10 indicates that the rate of photocatalytic degradation is not much affected by temperature, showing only little increase as the temperature is increased. Values of QY, TN, and TF and the percent

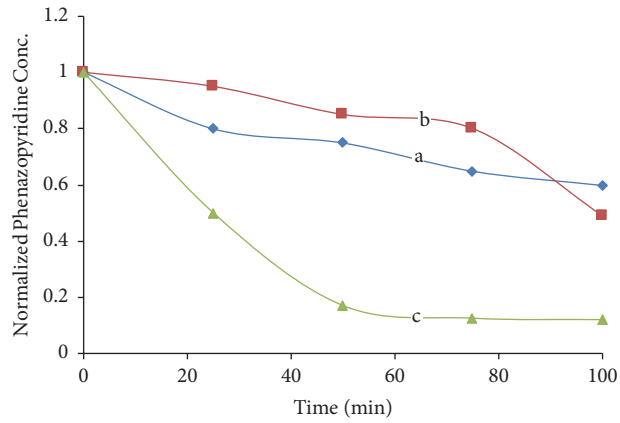

Figure 11: Effect of catalyst concentration on phenazopyridine degradation at room temperature: (a) 0.050 g, (b) 0.075 g, and (c) 0.15 g.

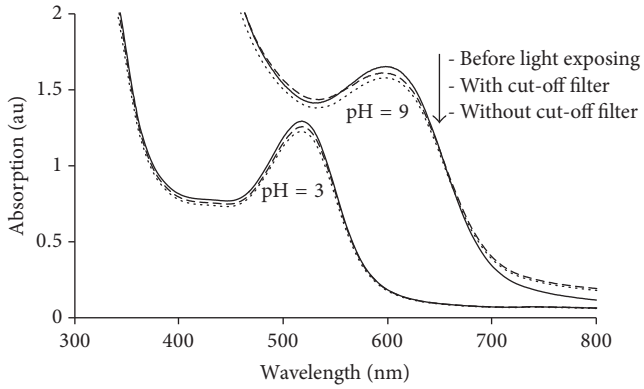

Figure 12: Electronic absorption spectra measured for *AC/TiO*$_2$/*Anthocyanin* under light at different pH values.

of degradation only slightly increased with increasing the temperature, Table 2.

The activation energy (E_{act}) value was calculated using plots of ln (initial rate) versus ($1/T$). The value of E_{act} was relatively small (~9 kJ/mol). This explains the observed small effect of temperature on reaction rate, as shown in Table 2. The results observed here are thus consistent with earlier literature reports, where temperature shows little effect on photocatalytic processes [57].

3.3.4. Effect of Catalyst Concentration. The effect of catalyst concentration on photodegradation reaction progress was studied using different loadings of *AC/TiO*$_2$*/Anthocyanin* catalyst, namely, 0.05 g, 0.075 g, and 0.15 g. The relation between catalyst concentration and photodegradation rate is shown in Figure 11.

As shown in Figure 11, increasing the catalyst amount increased photodegradation progress. This is understandable, as the number of catalytically active sites increases with catalyst concentration. These results are consistent with the earlier literature [57, 62]. Values of percent degradation, turnover number, turnover frequency, and quantum yield are summarized in Table 2.

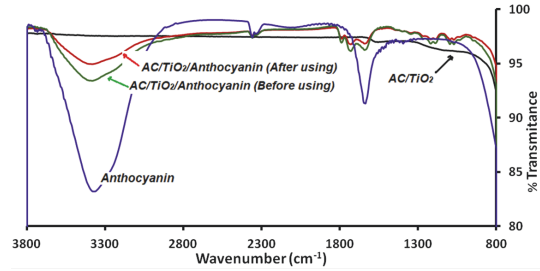

Figure 13: FT-IR spectra measured for *Anthocyanin, AC/TiO*$_2$, and *AC/TiO*$_2$*/Anthocyanin* before and after using.

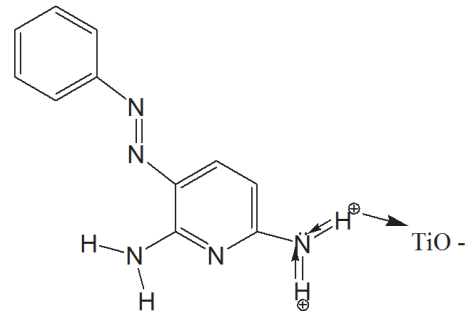

Scheme 5: A schematic structure showing how adsorption of phenazopyridine on TiO_2 surface is favored at higher pH.

3.3.5. Catalyst Stability. The stability of the sensitizing dye under the reaction working conditions was studied here. Figure 12 shows that the no loss in anthocyanin was observed after 100 min exposure of *AC/TiO*$_2$*/Anthocyanin* catalyst to light. There is only slight lowering in electronic absorption spectral intensity for catalyst sample exposed to light with and without cut-off filter in both acidic and basic media. This confirms the anthocyanin stability to photodegradation under catalytic experimental conditions. The results confirm the advantage of using anthocyanin as a sensitizer for photodegradation of water contaminants.

The FT-IR results, Figure 13, show that the catalyst retains its anthocyanin molecules on its surface after the photodegradation reaction cessation. Anthocyanin characteristic IR bands are shown in the regions at ~1640 cm^{-1} and ~3400 cm^{-1}, like earlier reports [63, 64]. These bands are shown for *AC/TiO*$_2$*/Anthocyanin* before and after the reaction, which indicates that the dye remains intact with the TiO_2 surface during the reaction process. The stability of the dye makes the catalyst useful after recovery.

Catalyst Recovery and Reuse. The unsupported TiO_2 particles could not be recovered by decantation. This is understandable due to the nanoscale nature of these particles which prevents their easy recovery. The AC supported catalyst was easy to isolate by simple decantation. The supported catalyst systems have thus been recovered and reused as described here.

Catalyst recovery and reuse results are presented in Figure 13. The fresh sample of the catalyst caused degradation of up to 91% of the phenazopyridine contaminant in

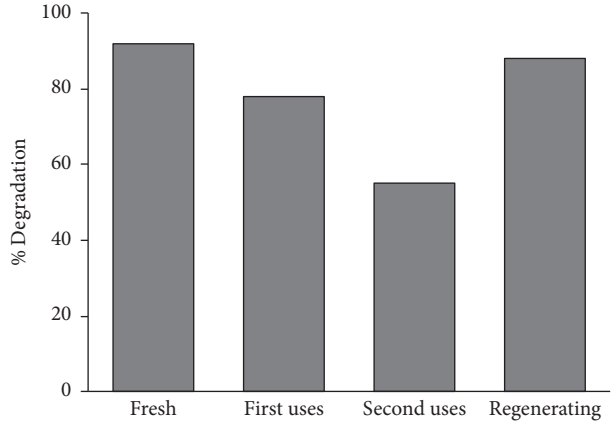

FIGURE 14: The *AC/TiO$_2$/Anthocyanin* reuse results of photodegradation of phenazopyridine for fresh, 1st uses, 2nd uses, and after regenerating with fresh anthocyanin.

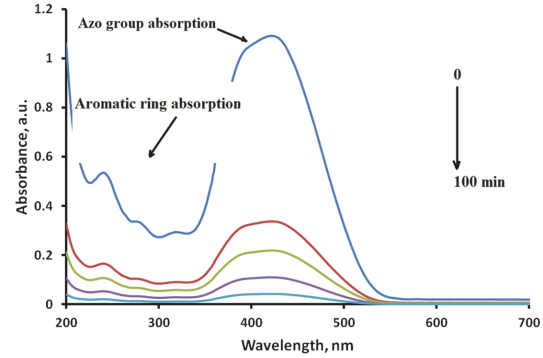

FIGURE 15: Electronic absorption spectra measured for phenazopyridine solutions after different reaction times.

100 min. The first recovered catalyst degraded about 78% of the phenazopyridine solution, while after second recovery the catalyst degraded about 55% of the contaminant. The lowering in recovered catalyst efficiency is presumably due to loss of the sensitizer. Regenerating the recovered catalyst, by adding anthocyanin, significantly enhances its activity. About 88% of the contaminant is degraded by the regenerated recovered catalyst, as shown in Figure 14.

Confirmation of Phenazopyridine Complete Mineralization. Photodegradation of organic contaminants may produce undesirable products. Phenazopyridine molecule contains an azo group that bridges two aromatic rings. The UV-visible spectrum of phenazopyridine has an absorption band in the visible region related to the azo group, and another one in the UV region for the aromatic rings. To confirm complete mineralization of phenazopyridine molecules by photodegradation, the remaining solution was studied by electronic absorption spectra in separate experiments. A solution of phenazopyridine (50 mL, 40 ppm) was mixed with 0.15 g AC/TiO_2/Anthocyanin catalyst and magnetically stirred in dark for 120 min. The reaction mixture was then exposed to solar simulated light as described above for different time durations. Aliquots were syringed out from the reaction mixture after different exposure times. Each sample was then centrifuged and analyzed by electronic absorption spectra in the range 200–800 nm. The spectra show the continued disappearance of the contaminant with photodegradation reaction time, as shown in Figure 15. After 100 min reaction time, the azo and aromatic rings completely disappeared from the reaction mixture. This confirms the complete degradation of the original contaminant by photodegradation. The study shows the feasibility of using the photocatalyst described here for complete removal of phenazopyridine from water solar simulated light.

The total organic carbon (TOC) in the photodegradation experiments is another evidence for complete mineralization of the contaminant. Two solutions of phenazopyridine (50 mL, 40 ppm) were mixed with 0.15 g *AC/TiO$_2$/Anthocyanin* catalyst and magnetically stirred in dark for 120 min. One mixture was exposed to light source as described above for 100 min, and the other was left in dark. The two mixtures were then analyzed for TOC. The experiment was repeated three times, and the average analysis results were as follows. The TOC for the mixture in the dark was 24 ± 3 (ppm), while for the irradiated mixture it was 4 ± 2 (ppm). The TOC results confirm the electronic absorption results discussed in Figure 15. Complete mineralization of the reacted phenazopyridine, by photodegradation, to gaseous minerals is evident. No organic matter is left from the reacted contaminant molecules.

4. Conclusion

Nanosize TiO_2 particles can be supported onto activated carbon and can be sensitized by anthocyanin molecules. The *AC/TiO$_2$/Anthocyanin* hybrid catalyst effectively catalyzes complete photodegradation of phenazopyridine contaminant in water under the visible and solar simulated lights. Anthocyanin is thus a promising replacement for other hazardous sensitizers based on synthetic quantum dot particles (such as CdS) or metal based molecules (such as Ru-compounds). The *AC/TiO$_2$/Anthocyanin* system can be readily recovered and reused for fresh contaminant photodegradation. The catalytic efficiency of the recovered TiO_2 catalyst system can be further enhanced by regeneration with a fresh anthocyanin dye.

Conflicts of Interest

The authors declare that there are no conflicts of interest regarding the publication of this paper.

Authors' Contributions

Hikmat S. Hilal supervised Fedaa Saleh thesis; Ahed H. Zyoud performed additional characterization analysis, more studies, and additional experiments. Ahed H. Zyoud and Hikmat S. Hilal undertook manuscript writing up and production. By virtue of their specialties, Muath H. Helal and Ramzi Shawahna managed pharmaceutical subjects and contributed in writing and literature surveying. All authors read and approved the final manuscript.

Acknowledgments

The authors wish to thank Dr. Guy Campet of ICMCB, University of Bordeaux, for measuring XRD and SEM. Financial support from Al-Maqdisi Project and from Union of Arab Universities is acknowledged. Parts of this work are based on Fedaa Saleh thesis, at An-Najah N. University.

References

[1] J. Grimm, D. Bessarabov, and R. Sanderson, "Review of electro-assisted methods for water purification," *Desalination*, vol. 115, no. 3, pp. 285–294, 1998.

[2] M. A. Shannon, P. W. Bohn, M. Elimelech, J. G. Georgiadis, B. J. Marīas, and A. M. Mayes, "Science and technology for water purification in the coming decades," *Nature*, vol. 452, no. 7185, pp. 301–310, 2008.

[3] S. A. A. Jahn, Traditional water purification in tropical developing countries; existing methods and potential application, Ed., German Agency for Technical Cooperation, 1981.

[4] H. J. Carlson, G. M. Ridenour, and C. F. McKhann, "Efficacy of standard purification methods in removing poliomyelitis virus from water," *American Journal of Public Health and the Nations Health*, vol. 32, pp. 1256–1262, 1942.

[5] R. D. Ambashta and M. Sillanpää, "Water purification using magnetic assistance: a review," *Journal of Hazardous Materials*, vol. 180, no. 1–3, pp. 38–49, 2010.

[6] I. Ali and V. K. Gupta, "Advances in water treatment by adsorption technology," *Nature Protocols*, vol. 1, no. 6, pp. 2661–2667, 2006.

[7] Q. Jiuhui, "Research progress of novel adsorption processes in water purification: a review," *Journal of Environmental Sciences*, vol. 20, pp. 1–13, 2008.

[8] K. Ikehata, N. Jodeiri Naghashkar, and M. Gamal El-Din, "Degradation of aqueous pharmaceuticals by ozonation and advanced oxidation processes: A review," *Ozone: Science & Engineering*, vol. 28, no. 6, pp. 353–414, 2006.

[9] J.-Y. Li, X. Jiang, L. Lin, J.-J. Zhou, G.-S. Xu, and Y.-P. Yuan, "Improving the photocatalytic performance of polyimide by constructing an inorganic-organic hybrid ZnO-polyimide core-shell structure," *Journal of Molecular Catalysis A: Chemical*, vol. 406, pp. 46–50, 2015.

[10] K. Rajalakshmi, *Photocatalytic Reduction of Carbon dioxide in conjunction with decomposition of water on oxide semiconductor surfaces*, Indian Institute of Technology, Madras, India, 2011.

[11] O. Carp, C. L. Huisman, and A. Reller, "Photoinduced reactivity of titanium dioxide," *Progress in Solid State Chemistry*, vol. 32, no. 1-2, pp. 33–177, 2004.

[12] S. S. Srinivasan, J. Wade, and E. K. Stefanakos, "Visible light photocatalysis via CdS/ TiO_2 nanocomposite materials," *Journal of Nanomaterials*, vol. 2006, Article ID 87326, 7 pages, 2006.

[13] A. L. Linsebigler, G. Q. Lu, and J. T. Yates Jr., "Photocatalysis on TiO_2 surfaces: principles, mechanisms, and selected results," *Chemical Reviews*, vol. 95, no. 3, pp. 735–758, 1995.

[14] C. Philippopoulos and M. Nikolaki, *Photocatalytic processes on the oxidation of organic compounds in water*, INTECH Open Access Publisher, 2010.

[15] J. N. Bhakta and Y. Munekage, "Degradation of Antibiotics (Trimethoprim and Sulphamethoxazole) Pollutants Using UV and TiO_2 in Aqueous Medium," *Modern Applied Science (MAS)*, vol. 3, no. 2, 2009.

[16] L. L. Costa and A. G. S. Prado, "TiO_2 nanotubes as recyclable catalyst for efficient photocatalytic degradation of indigo carmine dye," *Journal of Photochemistry and Photobiology A: Chemistry*, vol. 201, no. 1, pp. 45–49, 2009.

[17] K. Hilgenkamp, *Environmental Health: Ecological Perspectives*, Jones & Bartlett Learning, 2006.

[18] R. Kopf, "State-of-the-Art Program on Compound Semiconductors XXXVI, and Wide Bandgap Semiconductors for Photonic and Electronic Devices and Sensors II," in *Proceedings of the International Symposia, in, The Electrochemical Society*, 2002.

[19] C. Di Valentin, G. Pacchioni, A. Selloni, S. Livraghi, and E. Giamello, "Characterization of paramagnetic species in N-doped TiO_2 powders by EPR spectroscopy and DFT calculations," *The Journal of Physical Chemistry B*, vol. 109, no. 23, pp. 11414–11419, 2005.

[20] J. Wang, D. N. Tafen, J. P. Lewis et al., "Origin of photocatalytic activity of Nitrogen-doped TiO_2 nanobelts," *Journal of the American Chemical Society*, vol. 131, no. 34, pp. 12290–12297, 2009.

[21] A. H. Zyoud, N. Zaatar, I. Saadeddin et al., "CdS-sensitized TiO_2 in phenazopyridine photo-degradation: catalyst efficiency, stability and feasibility assessment," *Journal of Hazardous Materials*, vol. 173, no. 1–3, pp. 318–325, 2010.

[22] Y. Xie, G. Ali, S. H. Yoo, and S. O. Cho, "Sonication-assisted synthesis of CdS quantum-dot-sensitized TiO_2 nanotube arrays with enhanced photoelectrochemical and photocatalytic activity," *ACS Applied Materials & Interfaces*, vol. 2, no. 10, pp. 2910–2914, 2010.

[23] J. Zhu, D. Yang, J. Geng, D. Chen, and Z. Jiang, "Synthesis and characterization of bamboo-like CdS/TiO_2 nanotubes composites with enhanced visible-light photocatalytic activity," *Journal of Nanoparticle Research*, vol. 10, no. 5, pp. 729–736, 2008.

[24] S. Meng, J. Ren, and E. Kaxiras, "Natural dyes adsorbed on TiO_2 nanowire for photovoltaic applications: enhanced light absorption and ultrafast electron injection," *Nano Letters*, vol. 8, no. 10, pp. 3266–3272, 2008.

[25] A. Zyoud, N. Zaatar, I. Saadeddin et al., "Alternative natural dyes in water purification: anthocyanin as TiO_2-sensitizer in methyl orange photo-degradation," *Solid State Sciences*, vol. 13, no. 6, pp. 1268–1275, 2011.

[26] A. Zyoud and H. Hilal, "Investigation of curcumin as sensitizer for anatase TiO_2 nanoparticles in photodegradation of of phenazopyridine with visible light," *PhytoChem & BioSub Journal*, vol. 8, pp. 127–137, 2014.

[27] D. A. H. Hanaor and C. C. Sorrell, "Review of the anatase to rutile phase transformation," *Journal of Materials Science*, vol. 46, no. 4, pp. 855–874, 2011.

[28] S. Hao, J. Wu, Y. Huang, and J. Lin, "Natural dyes as photosensitizers for dye-sensitized solar cell," *Solar Energy*, vol. 80, no. 2, pp. 209–214, 2006.

[29] M. Grätzel, "Dye-sensitized solar cells," *Journal of Photochemistry and Photobiology C: Photochemistry Reviews*, vol. 4, pp. 145–153, 2003.

[30] A. Zyoud and H. Hilal, "Curcumin-sensitized anatase TiO2 nanoparticles for photodegradation of methyl orange with solar radiation," in *Proceedings of the 2013 1st International Conference and Exhibition on the Applications of Information Technology to Renewable Energy Processes and Systems, IT-DREPS 2013*, pp. 31–36, IEEE, May 2013.

[31] J. Drelich, E. Chibowski, D. D. Meng, and K. Terpilowski, "Hydrophilic and superhydrophilic surfaces and materials," *Soft Matter*, vol. 7, no. 21, pp. 9804–9828, 2011.

[32] S. Paria and K. C. Khilar, "A review on experimental studies of surfactant adsorption at the hydrophilic solid-water interface," *Advances in Colloid and Interface Science*, vol. 110, no. 3, pp. 75–95, 2004.

[33] R. Zhang and P. Somasundaran, "Advances in adsorption of surfactants and their mixtures at solid/solution interfaces," *Advances in Colloid and Interface Science*, vol. 123-126, pp. 213–229, 2006.

[34] W. Zheng, C. Sun, and B. Bai, "Molecular dynamics study on the effect of surface hydroxyl groups on three-phase wettability in oil-water-graphite systems," *Polymer*, vol. 9, no. 8, article no. 370, 2017.

[35] D. Ghosh and T. Konishi, "Anthocyanins and anthocyanin-rich extracts: Role in diabetes and eye function," *Asia Pacific Journal of Clinical Nutrition*, vol. 16, no. 2, pp. 200–208, 2007.

[36] A. d. M. Petersen, *Comportamento inibidor da corrosão de antocianinas na liga de alumínio 2024-T3*, 2016.

[37] W. Macyk, K. Szaciłowski, G. Stochel, M. Buchalska, J. Kuncewicz, and P. Łabuz, "Titanium(IV) complexes as direct TiO_2 photosensitizers," *Coordination Chemistry Reviews*, vol. 254, no. 21-22, pp. 2687–2701, 2010.

[38] M. N. Muniz, *Teaching Tools for Pedagogy at the Nanoscale: Towards the Understanding of Concepts Through Experience and Experimentation*, 2014.

[39] S. D. Kim, J. Cho, I. S. Kim, B. J. Vanderford, and S. A. Snyder, "Occurrence and removal of pharmaceuticals and endocrine disruptors in South Korean surface, drinking, and waste waters," *Water Research*, vol. 41, no. 5, pp. 1013–1021, 2007.

[40] D. W. Kolpin, E. T. Furlong, M. T. Meyer et al., "Pharmaceuticals, hormones, and other organic wastewater contaminants in US streams, 1999-2000: A national reconnaissance," *Environmental Science & Technology*, vol. 36, no. 6, pp. 1202–1211, 2002.

[41] A. Y.-C. Lin, T.-H. Yu, and C.-F. Lin, "Pharmaceutical contamination in residential, industrial, and agricultural waste streams: Risk to aqueous environments in Taiwan," *Chemosphere*, vol. 74, no. 1, pp. 131–141, 2008.

[42] B. Halling-Sørensen, S. N. Nielsen, P. F. Lanzky, F. Ingerslev, H. C. H. Lützhøft, and S. E. Jørgensen, "Occurrence, fate and effects of pharmaceutical substances in the environment—a review," *Chemosphere*, vol. 36, no. 2, pp. 357–393, 1998.

[43] F. T. Saleh, *Sensitization of semiconducting nano powder catalysts in photodegradation of medical drugs and microorganisms in water*, Master Thesis in Chemistry Science, Faculty of Graduate Studies, An-Najah National University, 2011.

[44] M. Rein, *Copigmentation reactions and color stability of berry anthocyanins*, University of Helsinki Helsinki, 2005.

[45] A. A. Abou-Arab, F. M. Abu-Salem, and E. A. Abou-Arab, "hysico-chemical properties of natural pigments (anthocyanin) extracted from Roselle calyces (Hibiscus subdariffa)," *Journal of American Science*, vol. 7, pp. 445–456, 2011.

[46] T. Suwandi, D. F. Suniarti, and S. W. Prayitno, "Effect of ethanol extract of Hibiscus sabdariffa L. calyx on Streptococcus sanguinis viability in vitro biofilm based on crystal violet," *Journal of Medicinal Plants Research*, vol. 33, pp. 2476–2482, 2013.

[47] Y. Bessekhouad, D. Robert, and J. V. Weber, "Preparation of TiO_2 nanoparticles by Sol-Gel route," *International Journal of Photoenergy*, vol. 5, no. 3, pp. 153–158, 2003.

[48] S. M. Sabry, "Adsorptive stripping voltammetric assay of phenazopyridine hydrochloride in biological fluids and pharmaceutical preparations," *Talanta*, vol. 50, no. 1, pp. 133–140, 1999.

[49] Y. Kim and S. Kang, "Effect of particle size on photoluminescence emission intensity in ZnO," *Acta Materialia*, vol. 59, no. 8, pp. 3024–3031, 2011.

[50] Y.-T. Chen, "Size effect on the photoluminescence shift in wide band-gap material: A case study of SiO~2-nanoparticles," *Tamkang Journal of Science and Engineering*, vol. 5, no. 2, pp. 99–106, 2002.

[51] C. S. Turchi and D. F. Ollis, "Photocatalytic degradation of organic water contaminants: mechanisms involving hydroxyl radical attack," *Journal of Catalysis*, vol. 122, no. 1, pp. 178–192, 1990.

[52] T. Wu, G. Liu, J. Zhao, H. Hidaka, and N. Serpone, "Photoassisted degradation of dye pollutants. V. Self-photosensitized oxidative transformation of *Rhodamine B* under visible light irradiation in aqueous TiO_2 dispersions," *The Journal of Physical Chemistry B*, vol. 102, no. 30, pp. 5845–5851, 1998.

[53] W. Li, D. Li, Y. Lin et al., "Evidence for the active species involved in the photodegradation process of methyl Orange on TiO_2," *The Journal of Physical Chemistry C*, vol. 116, no. 5, pp. 3552–3560, 2012.

[54] J. Yao and C. Wang, "Decolorization of methylene blue with TiO_2 sol via UV irradiation photocatalytic degradation," *International Journal of Photoenergy*, vol. 2010, Article ID 643182, 6 pages, 2010.

[55] S. Dutta, S. A. Parsons, C. Bhattacharjee, P. Jarvis, S. Datta, and S. Bandyopadhyay, "Kinetic study of adsorption and photodecolorization of reactive red 198 on TiO_2 surface," *Chemical Engineering Journal*, vol. 155, no. 3, pp. 674–679, 2009.

[56] A. R. Khataee, "Photocatalytic removal of C.I. Basic Red 46 on immobilized TiO2 nanoparticles: Artificial neural network modelling," *Environmental Technology*, vol. 30, no. 11, pp. 1155–1168, 2009.

[57] T. W. Kim, "Effect of pH and temperature for Photocatalytic degradation of organic compound on carbon-coated TiO_2," *Journal of Engineering and Technology*, vol. 3, pp. 193–198, 2010.

[58] N. Barka, A. Assabbane, A. Nounah, J. Dussaud, and Y. A. Ichou, "Photocatalytic degradation of methyl orange with immobilized TiO2 nanoparticles: effect of pH and some inorganic anions," *Physical and Chemical News*, vol. 41, pp. 85–88, 2008.

[59] T. Fossen, L. Cabrita, and O. M. Andersen, "Colour and stability of pure anthocyanins influenced by pH including the alkaline region," *Food Chemistry*, vol. 63, no. 4, pp. 435–440, 1998.

[60] P. S. Devi, M. Saravanakumar, and S. Moh, "The effects of temperature and pH on stability of anthocyanins from red sorghum (Sorghum bicolor) bran," *African Journal of Food Science*, vol. 6, pp. 567–573, 2012.

[61] H. S. Hilal, G. Y. M. Al-Nour, A. Zyoud, M. H. Helal, and I. Saadeddin, "Pristine and supported ZnO-based catalysts for phenazopyridine degradation with direct solar light," *Solid State Sciences*, vol. 12, no. 4, pp. 578–586, 2010.

[62] N. Barka, A. Assabbane, A. Nounah, and Y. A. Ichou, "Photocatalytic degradation of indigo carmine in aqueous solution by TiO_2-coated non-woven fibres," *Journal of Hazardous Materials*, vol. 152, no. 3, pp. 1054–1059, 2008.

[63] H. Chang, M. Kao, T. Chen, C. Chen, K. Cho, and X. Lai, "Characterization of natural dye extracted from wormwood and purple cabbage for dye-sensitized solar cells," *International Journal of Photoenergy*, vol. 2013, Article ID 159502, 8 pages, 2013.

[64] A. Soriano, P. M. Pérez-Juan, A. Vicario, J. M. González, and M. S. Pérez-Coello, "Determination of anthocyanins in red wine using a newly developed method based on Fourier transform infrared spectroscopy," *Food Chemistry*, vol. 104, no. 3, pp. 1295–1303, 2007.